Sites in human nuclei where damage induced by ultraviolet light is repaired: localization relative to transcription sites and concentrations of proliferating cell nuclear antigen and the tumour suppressor protein, p53

Dean A. Jackson[1], A. Bass Hassan[1], Rachel J. Errington[2] and Peter R. Cook[1],*

[1]CRC Nuclear Structure and Function Research Group, Sir William Dunn School of Pathology, University of Oxford, South Parks Road, Oxford OX1 3RE, UK
[2]Department of Physiology, University of Oxford, Parks Road, Oxford OX1 3PT, UK

*Author for correspondence

SUMMARY

The repair of damage induced in DNA by ultraviolet light involves excision of the damaged sequence and synthesis of new DNA to repair the gap. Sites of such repair synthesis were visualized by incubating permeabilized HeLa or MRC-5 cells with the DNA precursor, biotin-dUTP, in a physiological buffer; then incorporated biotin was immunolabelled with fluorescent antibodies. Repair did not take place at sites that reflected the DNA distribution; rather, sites were focally concentrated in a complex pattern. This pattern changed with time; initially intense repair took place at transcriptionally active sites but when transcription became inhibited it continued at sites with little transcription. Repair synthesis in vitro also occurred in the absence of transcription. Repair sites generally contained a high concentration of proliferating cell nuclear antigen but not the tumour-suppressor protein, p53.

Key words: p53, proliferating cell nuclear antigen, repair foci, repair synthesis, transcription foci

INTRODUCTION

Replication and transcription occur in distinct compartments in mammalian nuclei. For example, DNA precursors (e.g. bromo-deoxyuridine) are incorporated into ~150 discrete replication sites (Nakamura et al., 1986) and an RNA precursor (i.e. BrUTP) labels ~300-500 transcription foci (Jackson et al., 1993; Wansink et al., 1993). We show in the accompanying paper that the repair of damage induced in DNA by ultraviolet light (UV), which involves excision of damage and repair synthesis to fill the gap, is also compartmentalized (Jackson et al., 1994). HeLa or MRC-5 cells in G_1 phase were encapsulated in agarose microbeads (diam. ~50-150 μm), UV-irradiated, grown to allow repair to initiate and then permeabilized using streptolysin O in a physiological buffer. Encapsulation protects the fragile cells and allows thorough washing to remove endogenous pools of triphosphates, unbound antibodies and unincorporated fluorochromes. The physiological buffer maintains levels of RNA and DNA synthesis at essentially in vivo rates (Jackson et al., 1988); if polymerases had aggregated artifactually, levels should fall. Next, the permeabilized cells were incubated with biotin-dUTP to label repair sites and fixed using conditions that preserve the native (i.e. unfixed) pattern of S phase replication foci (Hassan and Cook, 1993). Finally, sites containing incorporated biotin were immunolabelled with fluorescent tags. We observed many small fluorescent foci; each one must contain many different

repair patches concentrated in a local compartment to give sufficient signal to be detected.

This approach allows visualization of repair synthesis at the global, rather than the molecular, level and opens up the possibility of seeing whether activities suggested to play a role in repair are indeed found at the active site of repair. Therefore we investigated whether repair sites were transcriptionally active and if they contained two possible components of the repair machinery, proliferating cell nuclear antigen (PCNA; Shivji et al., 1992) and the tumour-suppressor protein, p53 (Lane, 1992; Zambetti and Levine, 1993).

MATERIALS AND METHODS

Variations from the conditions used in the accompanying paper (Jackson et al., 1994) are described below

The effects of transcription on repair in vitro (see Fig. 7C) were analysed as follows. Encapsulated cells were lysed, mock- or UV-irradiated (40 J/m²), incubated (30 minutes; 33°C) in PB with or without the triphosphates required for transcription (i.e. 100 μM CTP, GTP and UTP plus $MgCl_2$ to maintain equimolar concentrations of triphosphates and Mg^{2+}). Next, samples were rewashed 3× in PB, reincubated with NTPs, dNTPs and [32P]dTTP, and the rate of incorporation of [32P]dTTP was measured. α-Amanitin (20 μg/ml) was added to some samples prior to incubations with NTPs and radiolabel. Omission of NTPs and addition of α-amanitin reduce transcription by mock-irradiated controls to 0 and 35% (not shown).

Sites of repair and transcription were colabelled using 50 µM BrUTP (Sigma; replaces UTP) and 25 µM biotin-16-dUTP, the MgCl$_2$ concentration was adjusted to maintain equimolarity of Mg^{2+} with triphosphates, all solutions used after lysis were treated with diethylpyrocarbonate to eliminate RNases, and RNAsin (Amersham) was added during incubations with antibodies and subsequent washes to final concentrations of 25 and 2.5 units/ml, respectively. Then sites containing incorporated biotin and Br were co-detected by incubation with the goat anti-biotin antibody described in the accompanying paper, washing 4×, incubation with a mouse monoclonal anti-bro-modeoxyuridine IgG that cross-reacts with BrRNA (Boehringer; 2 µg/ml; 16 hours; 4˚C; Jackson et al., 1993), washing 4×, incubation (4 hours; 4˚C) with a donkey anti-goat Ig conjugated with FITC (Jackson Labs; 1/500) plus a donkey anti-mouse Ig conjugated with Texas Red (Jackson Labs; 1/500 dilution), and rewashing 4×. Repair sites and p53, or repair sites and PCNA, were co-detected by succes-sive incubations with the goat anti-biotin antibody as above, a mouse monoclonal IgG anti-p53 (DO1 from David Lane; 1/500 dilution 1/500; 16 hours; 0˚C) or a mouse monoclonal anti-PCNA antibody (PC-10, of Waseem and Lane, 1990, from Oncogene Science; dilution 1/50; 16 hours; 0˚C), and the FITC- and Texas Red-conjugated anti-bodies as above. Methanol fixation was used prior to PCNA detection.

UV-induced damage was detected using a polyclonal rabbit antiserum raised against DNA irradiated with UV-C (McCready and Cox, 1993). Encapsulated cells were irradiated (40 J/m^2), immediately permeabilized (10 minutes, 0˚C) in PB plus 0.5% Triton X-100, washed 4× in PB (10 vol.), incubated (4 hours; 0˚C) with an equal volume of pre-absorbed antiserum (1000× dilution of original serum prepared by two incubations of 1 hour at 4˚C with an equal volume of 1/250 dilution of original antiserum with encapsulated, Triton-lysed HeLa cells at 10^7/ml), rewashed 4×, incubated (16 hours; 0˚C) with a FITC-conjugated donkey anti-rabbit IgG (Jackson Labs; 1/500 dilution) and rewashed 4×.

Digital images were captured using a Hamamatsu charge-coupled device (CCD; C4742; 1000×1018 pixel; −40˚C Peltier-cooled) attached to the Axiophot (Optivar 1.25-1.6×; ×100 oil-immersion lens; NA 1.3). An MRC 600 laser-scanning confocal microscope (Bio-Rad) fitted with an argon-ion laser (λ = 514) attached to Nikon
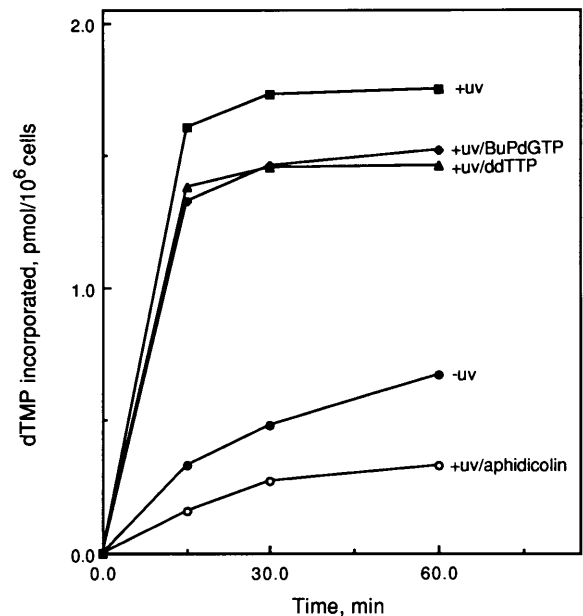

Fig. 1. UV irradiation stimulates DNA synthesis by HeLa cells in G$_1$. Encapsulated cells were mock- or UV-irradiated (40 J/m^2; indicated by ±UV), incubated for 1 hour in growth medium, permeabilized with streptolysin O and the rate of incorporation of [^{32}P]dTTP into acid-insoluble material was measured. In some cases 5 µM butylphenyl-dGTP (BuPdGTP), 20 µM ddTTP or 10 µg/ml aphidicolin were added 10 minutes before addition of [^{32}P]dTTP.

Diaphot inverted microscope (×60 oil-immersion objective; NA 1.4) was also used to collect 8× 1 µm optical slices through labelled nuclei. Images were contrast-stretched, median-filtered (3×3) and images from the green and red channels were pseudo-coloured and merged
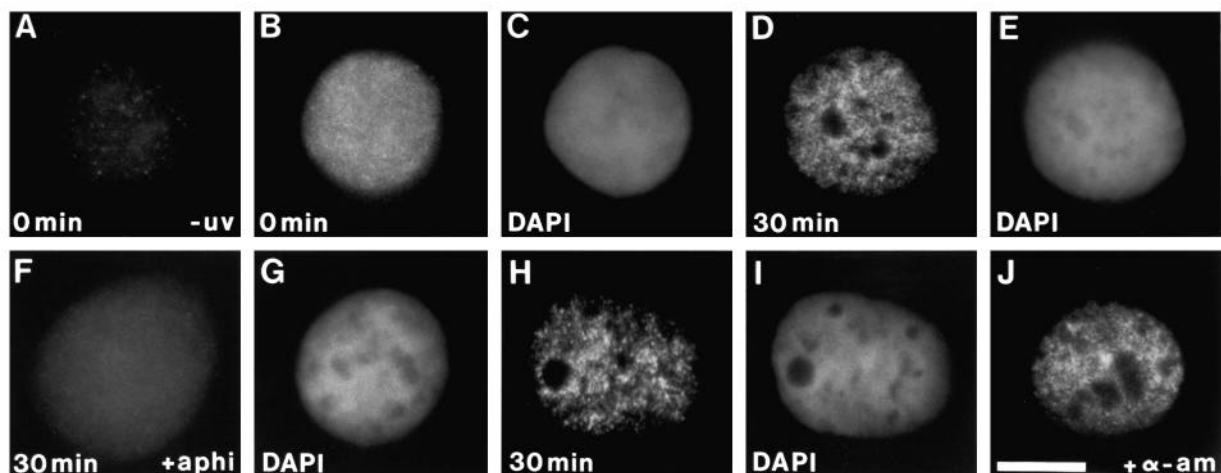

Fig. 2. Visualization of sites where UV-induced damage is introduced (A-C) and repaired (D-J). (A-C) Encapsulated HeLa cells were UV-irradiated (40 J/m^2), lysed immediately (0 minutes), and introduced damage was indirectly immunolabelled. (A) Which is unirradiated (−UV), was over-exposed to show background. (C) DAPI-staining of B. (D-I) Encapsulated HeLa (D-G) or MRC-5 (H,I) cells were UV-irradiated (40 J/m^2), grown for 30 minutes to allow repair to initiate (30 minutes), lysed, incubated for 15 minutes with biotin-dUTP and sites containing incorporated biotin were indirectly immunolabelled. (E,G,I) DAPI staining of cells on the left. (F) 20 µg/ml aphidicolin was added 10 minutes before addition of biotin-dUTP (+aphi); the photograph was over-exposed to show background in nucleus and cytoplasm. (J) Encapsulated HeLa cells were first lysed, UV-irradiated (40 J/m^2), incubated for 30 minutes with biotin-dUTP and sites containing incorporated biotin were indirectly immunolabelled; 20 µg/ml α-amanitin was added 10 minutes before addition of biotin-dUTP (+α-am). Bar, 5 µm.

(16-bit) using Adobe Photoshop. Various controls have been presented elsewhere that demonstrate: (i) specificity of labelling; (ii) lack of cross-labelling of DNA by BrUTP or RNA by biotin-dUTP; and (iii) lack of bleed-through between channels (Jackson et al., 1993, 1994; Hozák et al., 1993; Hassan and Cook, 1993; Hassan et al., 1994). Labelling levels were adjusted so that there was no detectable nuclear signal above noise in the appropriate channel if either BrUTP or biotin-dUTP was omitted during incubation with triphosphates. DNase treatment removes almost all repair foci (Jackson et al., 1994) and an example of lack of both cross-labelling and bleed-through is illustrated in Fig. 6A.

RESULTS

The effects of inhibitors on repair synthesis in vitro

HeLa cells in G_1 were UV-irradiated (40 J/m^2), grown to allow repair to initiate, permeabilized and incubated with [^{32}P]dTTP using a sub-optimal concentration of triphosphates. This dose is, in the biological context, extremely high; it reduces cloning efficiency to <1% (not shown) and introduces one endonuclease-sensitive site every ~5 kb (Williams and Cleaver, 1979; see also accompanying paper). Mock-irradiated cells incorporate label at a low, but detectable, rate (Fig. 1, −UV), which is probably due to the 0.4% contaminating S phase cells, some mitochondrial DNA synthesis and perhaps repair of existing damage (Jackson et al., 1994). UV irradiation increases incorporation (Fig. 1, +UV). The initial rate declines rapidly because the dTTP concentration allows rapid elongation and completion of the short repair patch (Jackson et al., 1994). UV-induced incorporation, plus some background synthesis, is sensitive to aphidicolin, but relatively insensitive to 5 μM butylphenyl-dGTP (BuPdGTP) or 20 μM ddTTP (Fig. 1); this profile is consistent with the UV-induced activity being polymerase δ (and/or ε; Kornberg and Baker, 1992) and implicates PCNA, a component of polymerase δ, in repair.

The distribution of damage in DNA

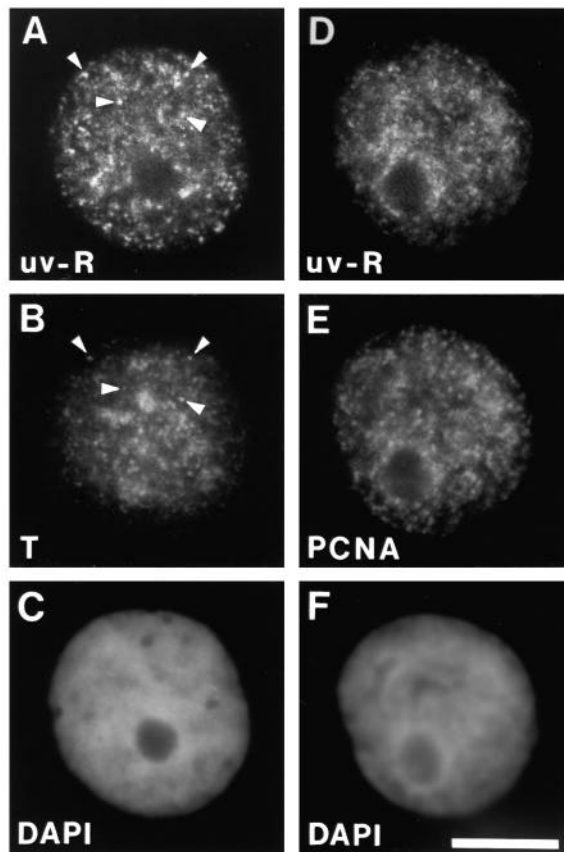We next investigated how irradiation deposited damage in

Fig. 3. Localization of repair sites with transcription sites and those containing PCNA. (A-C) Encapsulated HeLa cells were irradiated (40 J/m^2), grown for 30 minutes, permeabilized, incubated with biotin-dUTP plus BrUTP, sites of incorporation were indirectly immunolabelled with FITC (biotin-dUTP) and Texas Red (BrUTP) and one cell was photographed. (A, B and C) Illustrate repair replication (UV-R; FITC), transcription (T; Texas Red) and DAPI, respectively. (D-F) As A, except that cells were incubated with biotin-dUTP alone before sites of incorporation were labelled with FITC, and those containing PCNA with Texas Red. (A, B and C) Illustrate repair replication (UV-R; FITC), PCNA (Texas Red) and DAPI. Arrowheads indicate overlapping foci. Bar, 5 μm.
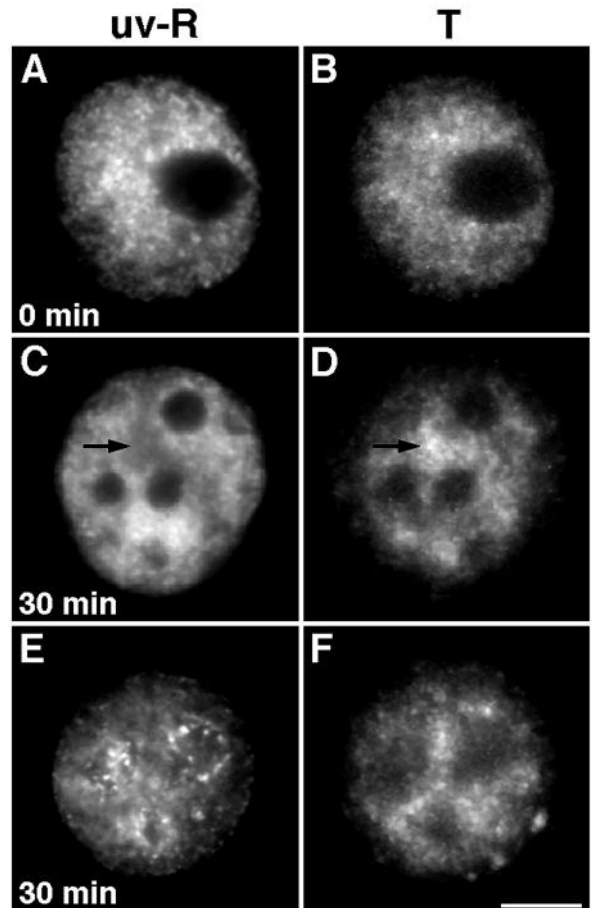

Fig. 4. Localization of sites of repair and transcription in the same cells. Encapsulated HeLa cells were irradiated (40 J/m^2), grown for 0 or 30 minutes, permeabilized, incubated with biotin-dUTP plus Br-UTP and sites of incorporation were indirectly immunolabelled with FITC (biotin-dUTP) and Texas Red (Br-UTP). Pairs of images of three cells were collected through green (repair replication; UV-R) and red filters (transcription; T) using a CCD camera. Dark areas are nucleoli. In C and D, arrows point to poorly repairing but actively transcribing regions, respectively. Bar, 5 μm.

nuclei by indirect immunofluorescence using an antibody raised against UV-irradiated DNA; ~2/3 of its activity is directed against thymine dimers and ~1/3 against 6-4 photoproducts (McCready and Cox, 1993). It stained nuclei of UV-irradiated HeLa cells (Fig. 2B) more intensely than mock-irradiated controls (Fig. 2A; this deliberate overexposure accentuates the background) and the pattern of staining was slightly more granular than that given by DAPI (Fig. 2C) or by antibodies directed against histones (not shown); damage seemed to be locally concentrated above a general background. This probably reflects the accessibility of antibody to different targets and perhaps the preferential introduction of 6-4 photoproducts into non-nucleosomal DNA (Mitchell et al., 1990; Sage, 1993) coupled with a concentration of transcribed genes into foci (Jackson et al., 1993; Wansink et al., 1993).

Visualization of sites of repair synthesis

Sites of repair were visualized as follows. G_1 cells were irradiated, grown to allow repair to initiate, lysed and incubated with biotin-16-dUTP; sites containing incorporated analogue were then indirectly immunolabelled using an anti-biotin antibody. UV-irradiated nuclei were more intensely labelled (Fig. 2D; E shows DAPI-staining) than mock-irradiated controls (not shown) or those incubated with aphidicolin (Fig. 2F; this overexposure again accentuates background in both nucleus and cytoplasm). Fig. 2H illustrates repair foci in MRC-5 cells (Fig. 2I shows DAPI staining). Incorporated biotin was not diffusely spread throughout nuclei like DAPI-staining material but focally concentrated in both cell types in extra-nucleolar regions. The foci are introduced in a dose-dependent manner and are removed by DNase treatment (Jackson et al., 1994). The pattern was simpler than that of unrepaired damage detected by the antibody directed against UV-irradiated DNA (compare Fig. 2B with D); taken at face value, this suggests that repair incorporation does not reflect the concentration of damage. However, differences in antibody accessibility could again underlie the different patterns.

Co-localization of sites of repair and transcription

As repair patterns are reminiscent of transcription patterns (Jackson et al., 1993), and as the two processes share accessory proteins and so may be tightly coupled (Downes et al., 1993;
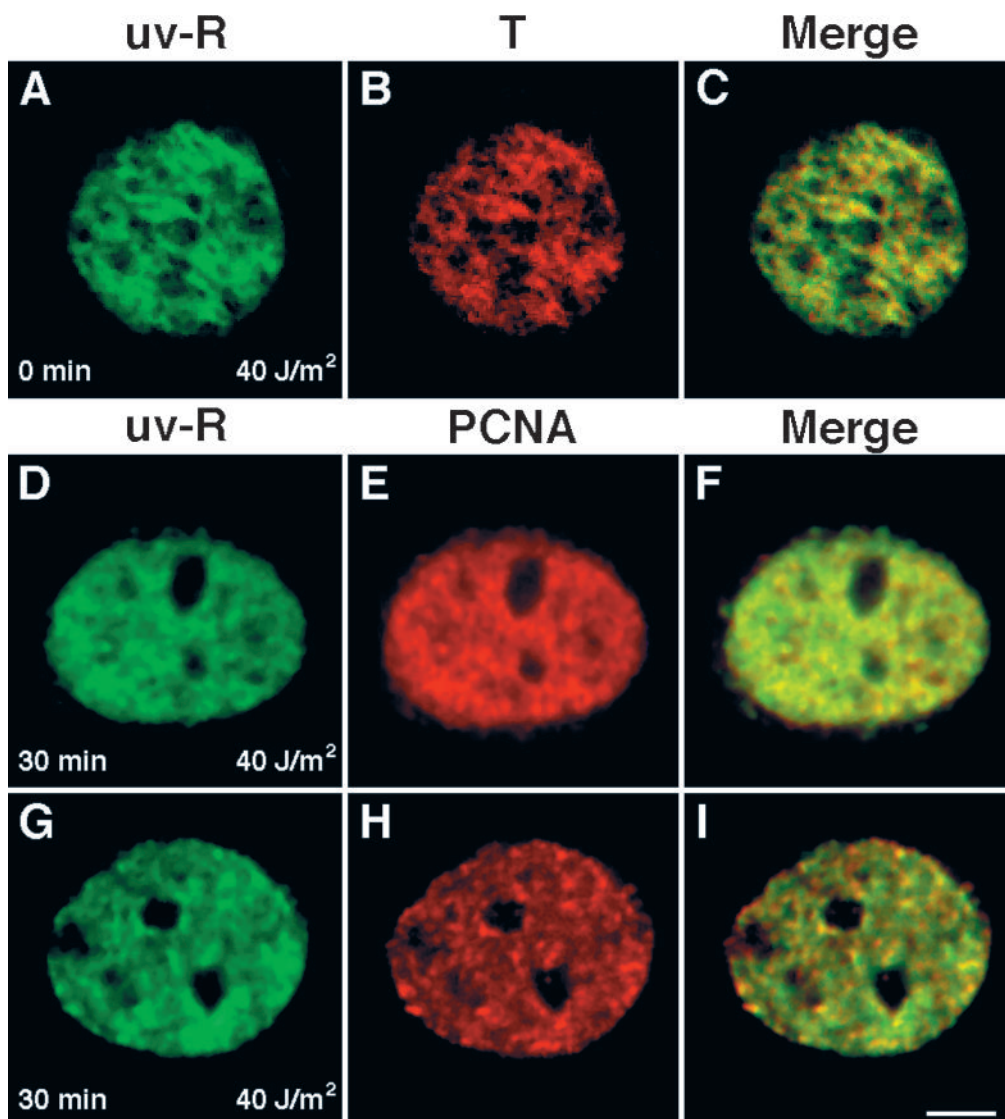

Fig. 5. Localization of sites of repair and transcription (A-C) and of repair and PCNA (D-I) by confocal microscopy. Encapsulated HeLa cells were irradiated (40 J/m²), grown for 0 or 30 minutes, lysed and sites of repair replication, transcription and PCNA were indirectly immunolabelled with FITC (biotin-dUTP) and Texas Red (Br-UTP and PCNA). Each row gives three different views of a central section through a cell. (A,D and G) Green channel, UV-induced replication (UV-R). (B,E and H) Red channel, transcription (T) or PCNA. (C,F and I) Merge of two images on left; yellow indicates where green overlaps red (see Fig. 6C for 'look-up' table). Bar, 5 μm.

Selby and Sancar, 1993; Bootsma and Hoeijmakers, 1993), we examined how closely the two patterns overlapped. G_1 HeLa cells were irradiated, grown for 30 minutes to allow repair to initiate, permeabilized, incubated with both biotin-dUTP and Br-UTP to label sites of repair and transcription simultaneously before the different sites were immunolabelled with FITC and Texas Red, respectively.

Sites of both UV-induced replication (UV-R) and transcription (T) were focal (Fig. 3A,B), unlike the DNA distribution (indicated by DAPI staining; Fig. 3C). In the particular cell illustrated, the two patterns are clearly different, although the textures are similar and some individual foci overlap (Fig. 3A,B; arrowheads point to overlapping foci). The dissimilarity of the patterns can be compared with the similarity of patterns given by repair and PCNA, a component of the repair machinery (Toschi and Bravo, 1988; Shivji et al., 1992); the two patterns are equally complex and overlapping (Fig. 3, D-F).

The cell shown in Fig. 3A-C is typical of the majority in the population, but others had different patterns with more or less overlap; the overlap depends upon a complex interplay between repair and transcription rates at different times and places. For example, if cells are irradiated (40 J/m^2) and grown for increasing periods before lysis, repair incorporation increases progressively to a maximum after 1 hour and then declines (Jackson et al., 1994). The rate of transcription declines concurrently with the initial increase; growth for 0, 10 or 60 minutes before lysis progressively reduces the rate of incorporation in vitro of $[^{32}P]$UTP into RNA to 95, 84 and 65%, respectively, of the rate with mock-irradiated controls (not shown). The average values obtained with cell populations hide wide variations visible in single cells, which incorporate different amounts of both biotin-dUTP and Br-UTP. Some examples of these differences photographed using a sensitive CCD camera are now given; the views are of whole cells and include out-of-focus flare, and so are comparable with photographs taken using conventional film.

Immediately after irradiation (i.e. before transcription is significantly inhibited) the texture of the patterns of repair and transcription are similar but the overall distribution of foci appears different (Fig. 4A,B). However, close inspection of the digital images in each channel shows that intense repair foci
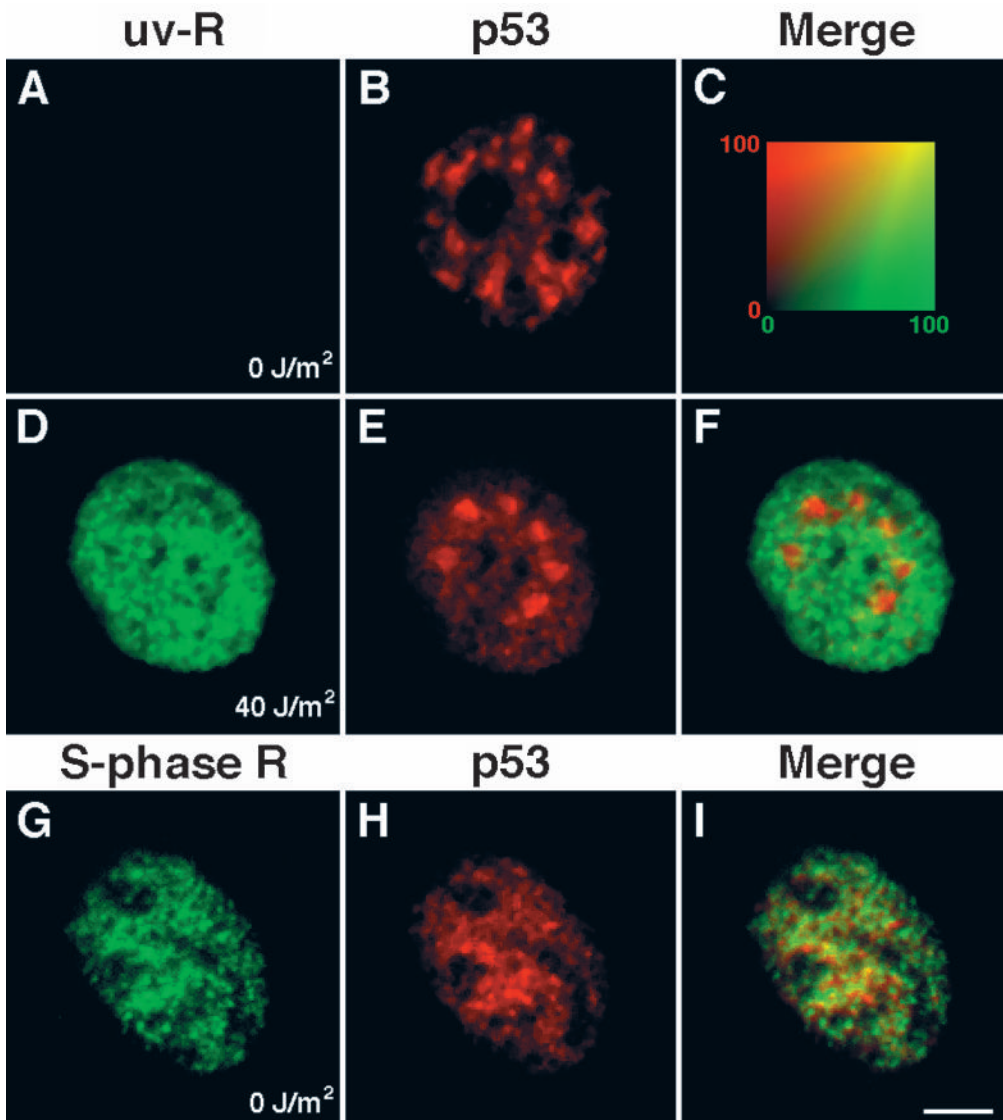

Fig. 6. The localization of sites of repair and p53 (A-F), and of S phase replication and p53 (G-I) by confocal microscopy. Encapsulated MRC-5 cells were mock- or UV-irradiated (40 J/m^2), grown for 1 hour, lysed and sites of repair or S phase DNA synthesis and p53 were indirectly immunolabelled with FITC (biotin) and Texas Red (p53). Each row gives three different views of the a central section through a cell. (A,D,G) Green channel, UV-induced replication (UV-R) or S phase replication (S phase R). (B,E,H) Red channel, p53. (C,F,I) Merge (merge of A plus B is not given as the resulting image is the same as B; instead a look-up table allows estimation of the relative amounts of green and red in a merge). The upper two cells were selected from a synchronized G_1 population and the lower cell from an unsynchronized population; the latter has the replication pattern typical of an early S phase cell (Hassan et al., 1994). Bar, 5 μm.

often, but not always, overlap transcription foci. As transcription becomes inhibited, the initially discrete repair foci become more diffuse (compare Fig. 4A with C) and the two patterns become quite different (compare Fig. 4C with D); this is confirmed by inspection of the digital images. Intensely repairing regions have little transcriptional activity and vice versa (Fig. 4C,D; arrows point to a region that is relatively inactive in repair but intensely transcribing). Later still, the overlap remains poor and repair sites become concentrated around nucleoli, reminiscent of the pattern of replication sites found during mid S phase (Nakamura et al., 1986; Hassan et al., 1994).

We next used the confocal microscope, which removes background 'flare', to analyse more carefully the degree of overlap between repair and transcription immediately after irradiation when transcription is hardly inhibited (Fig. 5A-C). The (green) repair pattern now coincides more perfectly with the (red) transcription pattern; overlap is indicated by yellow when the two images are merged (Fig. 5C). (Hassan et al. (1994) describe a graded series of patterns of different complexities that were obtained using the same equipment and conditions; these can be used to compare the extent of overlap.) The results in Figs 4 and 5A-C suggest that intense repair begins in transcriptionally active sites but the two patterns rapidly diverge as transcription is inhibited. Then, intense repair continues in regions where transcription is suppressed before it switches to new, and perhaps more heterochromatic, regions around nucleoli.

Repair sites contain PCNA

Confocal microscopy confirmed the close association seen earlier between repair and PCNA during different stages of this repair cycle. PCNA, initially present as a diffuse background in unirradiated cells, rapidly concentrates into foci after irradiation (Toschi and Bravo, 1988; Prosperi et al., 1993); the (green) repair pattern (Fig. 5D) then coincides with the (red) PCNA pattern (Fig. 5E), indicated by yellow in the merge (Fig. 5F). Later, when intense (green) repair occurs around nucleoli (red), PCNA also becomes peri-nucleolar (Fig. 5G-I). PCNA and repair change locations together, implying that they are tightly linked.

Repair sites are not particularly rich in p53

p53 is a tumour-suppressor protein that has been implicated in sensing damage in DNA, perhaps arresting cells in G_1 and so giving time for the damage to be repaired before duplication during S phase; in this way it could guard the genome from the results of the damage (reviewed by Lane, 1992; Zambetti and Levine, 1993). Therefore we used the confocal microscope to determine if p53 was present in repair and/or replication sites; MRC-5 cells used as antibodies to native p53 react poorly with HeLa cells.

p53 in unirradiated G_0 cells is concentrated in large (red) clumps that disaggregate to give a diffuse pattern during S phase (Fig. 6B,H). No repair is detectable in mock-irradiated cells (Fig. 6A). One hour after irradiation, the still large p53 clumps (Fig. 6E) are not particularly active in repair (Fig. 6D) and do not appear yellow in the corresponding merge (Fig. 6F). On entry into S phase, when the foci have dispersed, the p53 pattern becomes more like that given by S phase replication (Fig. 6G-I; colocalization is indicated by yellow in the

merge; replication and transcription patterns are colocalized at this stage; Hassan et al., 1994). These results show that p53 does not follow the repair pattern like PCNA; they are consistent with a redistribution of p53 from large stores in $G_0/1$ to sites of replication/transcription during early S phase, rather than to sites of repair. However, as this approach cannot distinguish between stored and active p53, we cannot exclude the possibility that a minority of the p53 is directly involved in repair.

A system for the initiation of repair in vitro

In the experiments described above, cells were irradiated and grown to allow repair to initiate in vivo before lysis and incorporation in vitro; therefore, the events required to initiate repair take place in an intact cell and the lysed cell is only required to elongate at established repair sites. However, lysed cells also initiate repair (e.g. see Dresler et al., 1982). For example, after lysis with streptolysin O, irradiation and incubation in vitro to allow initiation, irradiated cells incorporate [^{32}P]dTTP at a greater rate than mock-irradiated controls (Fig. 7A; compare – UV/SO with SO/+UV). This increased rate is lower and has different kinetics from that given by cells that have been allowed to initiate in vivo (Fig. 7A; compare +UV/SO with SO/+UV). It is dose dependent (Fig. 7B) and, unlike S phase replication (Jackson and Cook, 1986), it is enhanced by incubation at 33°C (not shown). Most lysed cells incorporate biotin-dUTP into foci that fluoresce less intensely than those found after initiation in vivo, although a minority fluoresce as brightly (see, for example, Fig. 2J). Clearly, lysed cells carry out, albeit less efficiently, all the steps in repair prior to elongation.

Repair synthesis is not inhibited by α-amanitin

We next used this in vitro system to determine if active transcription was required directly for repair. Encapsulated cells were lysed, irradiated and preincubated to allow repair to initiate with or without the triphosphates required for transcription; then the rate of incorporation of [^{32}P]dTTP into repair patches was measured. α-Amanitin was also added to some samples during both preincubation and incorporation of radiolabel. (The drug has no effect on repair synthesis in normal fibroblasts in vivo (Carreau and Hunting, 1992) but inhibits strand-specific removal of dimers from CHO cells (Christians and Hanawalt, 1992).) Mock-irradiated controls incorporated background levels (Fig. 7C, curve 1), which was slightly increased by preincubation with RNA precursors or α-amanitin (curves 2 and 3; this increase, though small, is reproducible). UV irradiation stimulated incorporation (curve 4), but there was again little additional effect of the RNA precursors or α-amanitin (curves 5 and 6). α-Amanitin also has no detectable effect on the incorporation of biotin-dUTP into repair foci (Fig. 2J). These results clearly show that repair occurs in this system in the absence of ongoing transcription by RNA polymerase II.

DISCUSSION

In vitro systems for repair

Several in vitro systems are available for studying UV-induced DNA synthesis at a lower than physiological concentration of
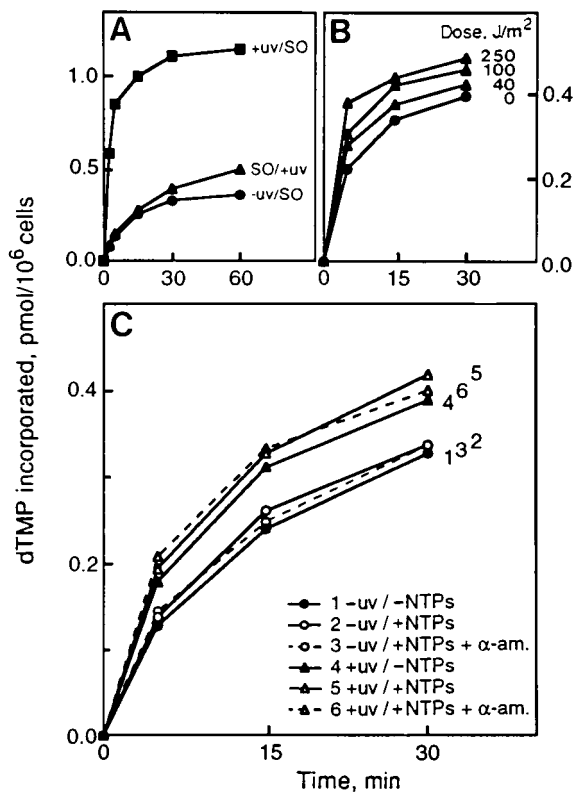
Fig. 7. Permeabilized HeLa cells can initiate repair. (A) Initiation of repair in vitro. Some encapsulated cells were mock- or UV-irradiated (40 J/m²), grown for 1 hour and lysed with streptolysin O (indicated by –UV/SO and +UV/SO); others were lysed, irradiated (40 J/m²) and incubated for 1 hour in PB at 0°C (indicated by SO/+UV). Then the rate of incorporation of [³²P]dTTP into acid-insoluble material was measured. (B) Dose-dependence. Encapsulated cells were lysed, UV-irradiated with different doses, incubated for 1 hour in PB at 0°C and the rate of incorporation of [³²P]dTTP was measured. (C) Initiation of repair occurs in the absence of NTPs and the presence of α-amanitin (details are given in Materials and Methods). Encapsulated cells were lysed, mock- or UV-irradiated (40 J/m²), incubated (30 minutes; 33°C) in PB with or without NTPs, washed and the rate of incorporation of [³²P]dTTP was measured. α-Amanitin (20 μg/ml) was added to some samples prior to incubation with NTPs and radiolabel.

salt (e.g. see Smith and Hanawalt, 1978; Ciarrocchi et al., 1979; Dresler et al., 1982; Wood, 1989). We have developed two additional systems that allow the use of more physiological conditions. In the first, which has been characterized in more detail by Jackson et al. (1994), G₁ cells are encapsulated in agarose microbeads, irradiated and grown to allow repair to initiate, before cells are permeabilized with streptolysin O in a physiological buffer; labelled precursors are then efficiently incorporated into DNA (Fig. 1). In the second, less efficient, system, encapsulated cells are first lysed and then UV-irradiated so that all the steps needed for UV-induced synthesis take place in vitro (Fig. 7A). The repair activities in these permeabilized cells are generally similar to those studied previously (e.g. see Dresler et al., 1982, 1988a,b). Although encapsulation is not necessary for either assay (Jackson et al., 1994), the lysed and now fragile cells can be washed repeatedly both to deplete

endogenous pools and to allow the kinds of experiment with many steps performed here.

Colocalizing complex patterns

Repair foci are small and numerous, and distributed in a complex pattern. This makes the determination of whether a repair pattern coincides with another complex pattern very difficult, even using a confocal microscope and sophisticated image analysis (e.g. see Taneja et al., 1992). Points ~200 nm apart in the *xy* plane can be resolved by confocal microscopy, but resolution in the *z* axis is poorer (i.e. ~500 nm at best). *z* Axis resolution can be improved by digitally deconvoluting information from serial sections, but this brings attendant problems (e.g. see Shaw et al., 1992). We have exploited elsewhere the better resolution in the *xy* plane to estimate how closely two patterns overlap (Hassan et al., 1994), but as repair patterns are even more complex than these we studied earlier, we use only a simple merge here to obtain a qualitative impression of overlap. These points should be borne in mind in the discussion that follows.

The role of transcription during the repair 'cycle'

Transcription could 'open' chromatin to allow access to the repair machinery and/or be involved directly in repair (Downes et al., 1993; Bootsma and Hoeijmakers, 1993). Immediately after irradiation, intense repair and transcription sites coincide (Fig. 5A-C), but as transcription becomes inhibited, repair continues in regions that are relatively transcriptionally inactive; later, repair becomes concentrated around nucleoli like replication sites seen during mid S phase (Fig. 4E). This implies that a repair cycle initiates in transcriptionally active regions but then continues independently of transcription. This independence from ongoing transcription is supported by studies in vitro; damage is repaired in the absence of RNA precursors and in the presence of α-amanitin, an inhibitor of RNA polymerase II (Fig. 7C).

The distribution of PCNA, a component of the repair polymerase (Shivji et al., 1992), follows the changing distribution of repair sites; early during the cycle it is spread extra-nucleolarly and later becomes concentrated around nucleoli (Fig. 5D-I).

Sites containing high concentrations of p53 are not particularly active in repair

The tumour-suppressor protein, p53, has been implicated in the cellular response to damage (Lane, 1992; Zambetti and Levine, 1993). This protein is concentrated in large clumps in G₀ MRC-5 cells, which disperse when cells begin to grow (Fig. 6B,H). One hour after irradiation, when repair activity is maximal, the still large p53 clumps are not particularly active in repair (Fig. 6D-F). Four hours after irradiation, when the clumps are almost completely dispersed and repair activity has declined, there is still little overlap (not shown). On entry into S phase the now dispersed p53 pattern becomes more like that given by S phase replication (Fig. 6G-I; at this stage, replication sites overlap transcription sites; Hassan et al., 1994). The p53 distribution does not follow repair like that of PCNA but p53 is redistributed from large G₀ stores to early S phase replication/transcription sites; however, we cannot exclude the possibility that a minority of p53 is directly involved in repair.

This approach has enabled us to see whether transcription,

PCNA and p53 colocalize with repair sites. In the future, it should allow us to screen which of the many other proteins that have been implicated in repair are also found at repair sites and whether mutants deficient in repair are defective in organizing repair centres.

REFERENCES

Bootsma, D. and Hoeijmakers, J. H. J. (1993). Engagement with transcription. *Nature* **363**, 114-115.

Carreau, M. and Hunting, D. (1992). Transcription-dependent and independent DNA excision repair pathways in human cells. *Mutat. Res.* **274**, 57-64.

Christians, F. C. and Hanawalt, P. C. (1992). Inhibition of transcription and strand-specific DNA repair by α-amanitin in Chinese hamster ovary cells. *Mutat. Res.* **274**, 93-101.

Ciarrocchi, G., Jose, J. G. and Linn, S. (1979). Further characterization of a cell-free system for measuring replicative and repair DNA synthesis with cultured human fibroblasts and evidence for the involvement of DNA polymerase a in DNA repair. *Nucl. Acids Res.* **7**, 1205-1219.

Downes, C. S., Ryan, A. J. and Johnson, R. T. (1993). Fine tuning of DNA repair in transcribed genes: mechanisms, prevalence and consequences. *BioEssays* **15**, 209-216.

Dresler, S. L., Roberts, J. D. and Lieberman, M. W. (1982). Characterization of deoxyribonucleic acid repair synthesis in permeable human fibroblasts. *Biochemistry* **21**, 2557-2564.

Dresler, S. L., Gowans, B. J., Robinson-Hill, R. M. and Hunting, D. J. (1988a). Involvement of DNA polymerase δ in DNA repair synthesis in human fibroblasts at late times after ultraviolet irradiation. *Biochemistry* **27**, 6379-6383.

Dresler, S. L., Frattini, M. G. and Robinson-Hill, R. M. (1988b). In situ enzymology of DNA replication and ultraviolet induced DNA repair synthesis in permeable human cells. *Biochemistry* **27**, 7247-7254.

Hassan, A. B. and Cook, P. R. (1993). Visualization of replication sites in unfixed human cells. *J. Cell Sci.* **105**, 541-550.

Hassan, A. B., Errington, R. J., White, N. S., Jackson, D. A. and Cook. P. R. (1994). Replication and transcription sites are colocalized in human cells. *J. Cell Sci.* **107**, 425-434.

Hozák, P., Hassan, A. B., Jackson, D. A. and Cook, P. R. (1993). Visualization of replication factories attached to a nucleoskeleton. *Cell* **73**, 361-373.

Jackson, D. A. and Cook, P. R. (1986). Different populations of DNA polymerase α in HeLa cells. *J. Mol. Biol.* **192**, 77-86.

Jackson, D. A., Yuan, J. and Cook, P. R. (1988). A gentle method for preparing cyto- and nucleo-skeletons and associated chromatin. *J. Cell Sci.* **90**, 365-378.

Jackson, D. A., Hassan, A. B., Errington, R. J. and Cook, P. R. (1993). Visualization of focal sites of transcription within human nuclei. *EMBO J.* **12**, 1059-1065.

Jackson, D. A., Balajee, A. S., Mullenders, L. and Cook, P. R. (1994). Sites in human nuclei where DNA damaged by ultraviolet light is repaired: visualization and localization relative to the nucleoskeleton. *J. Cell Sci.* **107**, 1745-1752.

Kornberg, A. and Baker, T. (1992). *DNA Replication*, second edition. W. H. Freeman, San Francisco.

Lane, D. P. (1992). p53, guardian of the genome. *Nature* **358**, 15-16.

McCready, S. and Cox, B. (1993). Repair of 6-4 photoproducts in *Saccharomyces cerevisiae*. *Mutat. Res. DNA Repair* **293**, 233-240.

Mitchell, D. L., Nguyen, T. D. and Cleaver, J. E. (1990). Nonrandom induction of pyrimidine-pyrimidone (6-4) photoproducts in ultraviolet-irradiated human chromatin. *J. Biol. Chem.* **265**, 5353-5356.

Nakamura, H., Morita, T. and Sato, C. (1986). Structural organisation of replicon domains during DNA synthetic phase in the mammalian nucleus. *Exp. Cell Res.* **165**, 291-297.

Prosperi, E., Stivala, L. A., Sala, E., Scovassi, A. I. and Bianchi, L. (1993). Proliferating cell nuclear antigen complex formation induced by ultraviolet irradiation in human quiescent fibroblasts as detected by immunostaining and flow cytometry. *Exp. Cell Res.* **205**, 320-325.

Sage, E. (1993). Distribution and repair of photolesions in DNA: genetic consequences and the role of sequence context. *Photochem. Photobiol.* **57**, 163-174.

Selby, C. P. and Sancar, A. (1993). Molecular mechanism of transcription-repair coupling. *Science* **260**, 53-58.

Shaw, P., Highett, M. and Rawlings, D. (1992). Confocal microscopy and image processing in the study of plant nuclear structure. *J. Microsc.* **166**, 87-97.

Shivji, M. K. K., Kenny, M. K. and Wood, R. D. (1992). Proliferating cell nuclear antigen is required for DNA excision repair. *Cell* **69**, 367-374.

Smith, C. A. and Hanawalt, P. C. (1978). Phage T4 endonuclease V stimulates DNA repair replication in isolated nuclei from ultraviolet-irradiated human cells, including xeroderma pigmentosum fibroblasts. *Proc. Nat. Acad. Sci. USA* **75**, 2598-2602.

Taneja, K. L., Lifshitz, L. M., Fay, F. S. and Singer, R. H. (1992). Poly(A) RNA codistribution with microfilaments: evaluation by in situ hybridization and quantitative digital imaging microscopy. *J. Cell Biol.* **119**, 1245-1260.

Toschi, L. and Bravo, R. (1988). Changes in cyclin/proliferating cell nuclear antigen distribution during DNA repair synthesis. *J. Cell Biol.* **107**, 1623-1628.

Wansink, D. G., Schul, W., van der Kraan, I., van Steensel, B., van Driel, R. and de Jong, L. (1993). Fluorescent labelling of nascent RNA reveals transcription by RNA polymerase II in domains scattered throughout the nucleus. *J. Cell Biol.* **122**, 283-293.

Waseem, N. H. and Lane, D. P. (1990). Monoclonal antibody analysis of the proliferating cell nuclear antigen (PCNA): structural conservation and detection of a nucleolar form. *J. Cell Sci.* **96**, 121-129.

Williams J. I. and Cleaver, J. E. (1979). Removal of T4 endonuclease V-sensitive sites from SV40 DNA after exposure to ultra-violet light. *Biochem. Biophys. Acta* **562**, 429-437.

Wood, R. D. (1989). Repair of pyrimidine dimer ultraviolet light photoproducts by human cell extracts. *Biochemistry* **28**, 8287-8292.

Zambetti, G. P. and Levine, A. J. (1993). A comparison of the biological activities of wild-type and mutant p53. *FASEB J.* **7**, 855-865.